

ASTROMESH™ DEPLOYABLE REFLECTORS FOR KU- AND KA-BAND COMMERCIAL SATELLITES

Mark W. Thomson
TRW Astro Aerospace
Carpinteria, California

Abstract

The potential for the AstroMesh deployable mesh reflectors to support Ku- and Ka-band commercial satellite missions is investigated. The focus of the work is on predicting reflector gain/loss for 6-meter aperture point designs operating at 14 GHz and 30 GHz. The use of RMS surface errors from both systematic and random sources for gain/loss estimates via Ruze is shown to be accurate, and grating lobe performance for the systematic components is shown to be acceptable. Mesh reflectivity performance is given and total loss estimates for viable Ku- and Ka-band point designs are presented.

Introduction

The Astro Aerospace (Astro) AstroMesh™ deployable reflector* has recently gained wide acceptance in the world of commercial satellites. The 12.25-meter aperture AstroMesh™ aboard Boeing Space System's Thuraya Satellite was successfully deployed in November 2000 and is operating flawlessly (Figure 1). Since then, the first of three 9-meter AstroMesh™ reflectors for the Astrium INMARSAT 4 satellite constellation was completed (Figure 2), and the manufacture of one 12-meter reflector for a Space Systems/Loral satellite being built for MBSAT has begun (Figure 3). Deliveries of flight units for both of the new programs are scheduled in 2002. INMARSAT 4 and Thuraya are L-band communications systems, and the MBSAT main antenna is an S-band broadcast system.

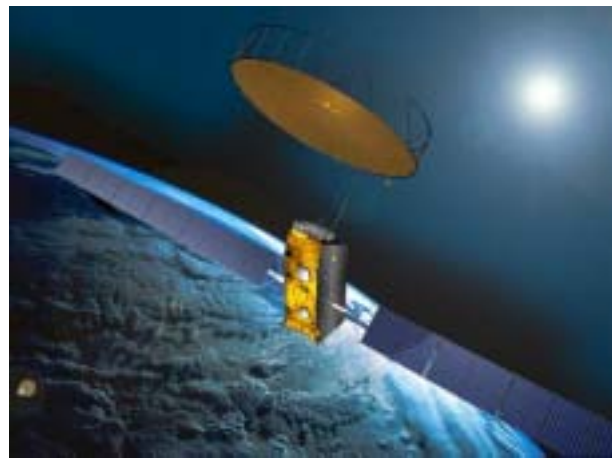


Figure 2. INMARSAT 4.

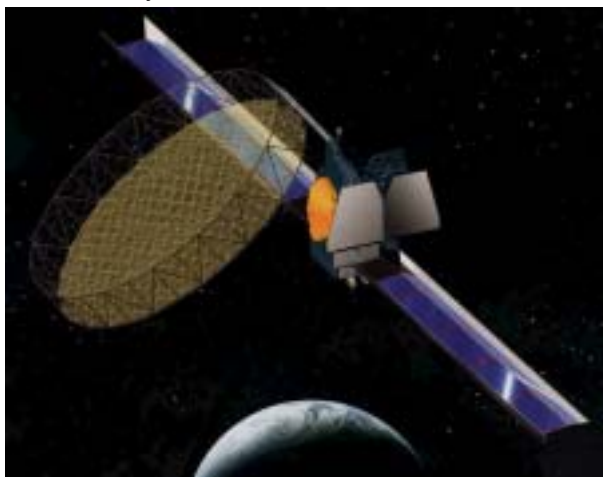


Figure 1. Thuraya Satellite

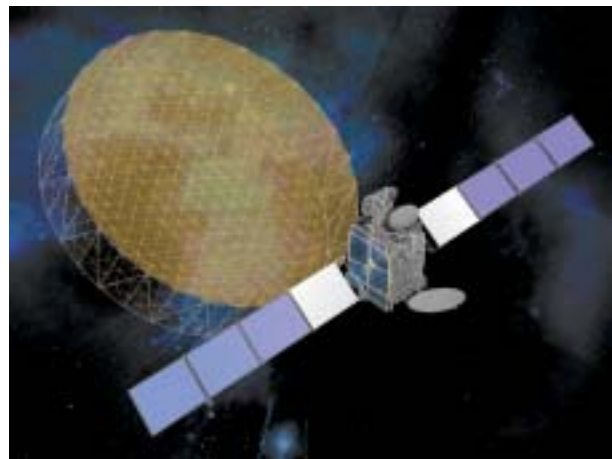


Figure 3. MBSAT

* U.S. Patent No. 5,680,145

It is apparent, however, that commercial satellites have compelling needs for deployable apertures that operate up to Ka-band. Broadcast applications can benefit from larger apertures to gain flatter coverage and to increase edge taper. Typical shaped Ku-band reflectors can be replaced with larger shaped AstroMesh™ surfaces to produce as much as a 3 dB increase in directivity with abrupt edge taper. This can provide a large reduction in satellite mass, power and cost for a given earth incident radiated power (EIRP), and maximize isolation.

Large deployable apertures may be requisite for certain geosynchronous broadband systems. Antennas that form numerous tightly focused spot beams for high reuse of frequency will support direct-to-home television with local programming or Internet satellites with ultra-high data rates and rural access. The stowed volume of the AstroMesh™ is small enough to allow several spot beam antennas to be mounted on a single spacecraft. The vastly increased capacity offered by such a payload would reduce user cost, which is a necessity for market success.

Fortunately, the performance of all AstroMesh™ flight reflectors has exceeded the existing L- and S-band requirements by substantial amounts. Confidence gained from the flight units has led to extensive analytical studies and IR&D projects at Astro. This work substantiates that the AstroMesh™ can deliver the high level of performance required for Ka-band payloads with apertures up to 6 meters, and for Ku-band payloads with apertures to 12 meters including shaped surfaces. This is possible with minor changes to the existing family of AstroMesh™ reflectors. These changes and how the resulting performance will be verified with engineering models in 2002 are described.

Reflector Requirements

Large aperture antennas have a considerable affect on satellite systems. Attitude control systems (ACS) require adequate deployed antenna stiffness to achieve the necessary beam-pointing precision. Because the antenna performance presented here involves half-power beam widths below 0.3 degrees, an unusually high level of deployed stiffness will be required. The reflector should also have low deployed mass and inertia, and require the smallest possible volume when stowed.

The focus of this discussion, however, is the prerequisite that a reflector must provide sufficient surface and pointing accuracy, thermal stability and RF reflectivity for an antenna system to perform properly in orbit. Reflectivity is a function of the mesh surface and the rest can be

summarized by W_{RSS} , the total root sum of squares (RSS) of all RMS[†] error contributions.

Commercial Ku- and Ka-Band satellite antenna link budgets typically require reflectors that conform to a specified shape to within $\lambda/50$ RMS or better. This value of W_{RSS} insures that peak gain loss, ΔG , remains below 0.3 dB as predicted by Ruze².

$$\Delta G = 10 \log_e^{(-4\pi W_{RSS}/\lambda)^2} \quad (1)$$

Ruze's derivation assumes random errors, but as we will see, equation (1) is also useful for estimating gain/loss from systematic error sources.

The goal for the reflector designs that are discussed is to control sidelobes and limit maximum gain loss from all sources to less than 0.30 dB. For the purpose of this study, thermal pointing errors are included in the contributions to total error from which gain losses are estimated using Ruze. Although this approach may not be suited to rigorous evaluations, it is useful for assessing the quality of an antenna surface and it's ability to achieve the intended mission. Frequencies of 14 GHz and 30 GHz will be used throughout to represent the Ku- and Ka-Bands respectively.

Related AstroMesh™ Background

The AstroMesh™ reflector has distinguished itself by providing unprecedented levels of performance for all the above requirements and more, including minimum cost and program schedule. It is lightweight and inherently stiff and precisely and it repeatably deploys the reflective mesh surface regardless of environments. As shown in Figure 4, the reflector consists of doubly curved geodesic truss structures called nets, made of stiff filamentary composites, placed back-to-back across a deployable rim truss made of graphite composite tubes and metallic fittings. Tension tie assemblies evenly apply approximately normal forces between the nets to permanently preload these stiff domes in tension across the truss. This forms a rigid drum-like structure that possesses exceptional structural efficiency, thermal dimensional stability and stiffness-to-weight ratios.

[†] All predictions and measurements of root mean square (RMS) error values are calculated using the Jet Propulsion Laboratory half-path length (HPL) error method given in Reference 1.

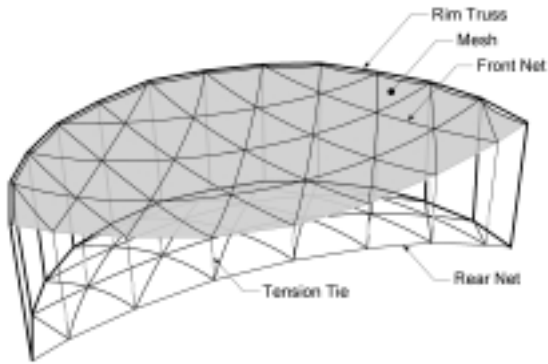


Figure 4. AstroMesh Reflector Design.

Highly RF reflective gold-plated molybdenum mesh is stretched across the convex side of the front net geodesic structure. This forms numerous mesh facets arranged in rings that approximate the required parabolic or other specialized shape. Mesh has been in orbit for more than 20 years on NASA's TDRS system. Qualified mesh designs are available for frequencies up to about 25 GHz with high reflectivity. Qualification is planned for a mesh developed to be viable through 40 GHz. All mesh designs have demonstrated low reflection losses without any preference for polarization directions in RF testing that was performed through 26 GHz, as discussed later.

The difference between the ideal surface and the faceted approximation is referred to as the systematic or faceting error. The AstroMesh™ has an unusual ability to maintain flat mesh facets with negligible mechanical pillowing (web bow due to mesh loads) in all environments, and to allow relatively high mesh tension. Although higher surface accuracy can be achieved by increasing the number of rings of facets, the inherent flatness and stability of AstroMesh™ facets allows a minimum number of them to be used. This is a key attribute on which the development of high frequency reflectors is based.

Development Status and Plans

AstroMesh™ technology is the culmination of seven generations of reflector hardware development over a period of 12 years. Reflectors from 2.5 to 12.25 meters have been built and tested to varying extents with a record of over 350 ground deployments and no failures to deploy. Three different flight designs will have been built and qualified by the end of 2002, and eight flight units will have been delivered to customers by mid 2003.

The 6-meter AstroMesh™ development model (DM) reflector shown in Figure 5 was built in 1994.

Although intended for L-band, it displays a total W_{RSS} surface accuracy of 0.6 mm from all sources and environments. Repeatability between deployments of the 6-meter DM and all other AstroMesh™ reflectors has been within the resolution of the measurement system[‡]. Cup-up versus cup-down surface contour measurements of the DM (2-g delta) were also within measurement resolution, evidence of a very stiff and stable reflector. Finally, structural and thermal tests spanning a range of 240°C have validated AstroMesh™ thermoelastic structural analysis methods.



Figure 5. 6-Meter Development Model.

The key to high-deployed stiffness for antenna-pointing precision using the AstroMesh™ is the deployment boom. A deployment boom configuration has been developed for the MBSAT 12-meter flight reflector system that will provide deployed reflector frequencies of up to 4.0 Hz when coupled to the edge-mounted, offset 6-meter reflector designs described herein. This frequency is usually adequate for the maintenance of beam pointing requirements at Ka-band during satellite body-steering control by the ACS.

[‡] The resolution of the 1994 measurements was ≤ 0.06 mm. The V-Stars™ video photogrammetry system, Geodetic Services, Inc., Melbourne FL, USA, is used for all surface measurements. Current equipment achieves up to 0.04 mm resolution on the 6-meter baseline.

The 6-meter DM reflector is, arguably, adequate for operating at the bottom of Ku-band. In order to meet the targeted performance, it is being modified in stages in 2002. A shaped surface for Ku-band coverage of Japan will be incorporated first. After testing, the shaped surface will be removed and replaced by a parabolic surface compatible with Ka-band. Tests at each stage include RF testing in a compact range for near-field performance verification and several deployments with photogrammetry to assess repeatability. The complete results will be available to prospective customers in 2003.

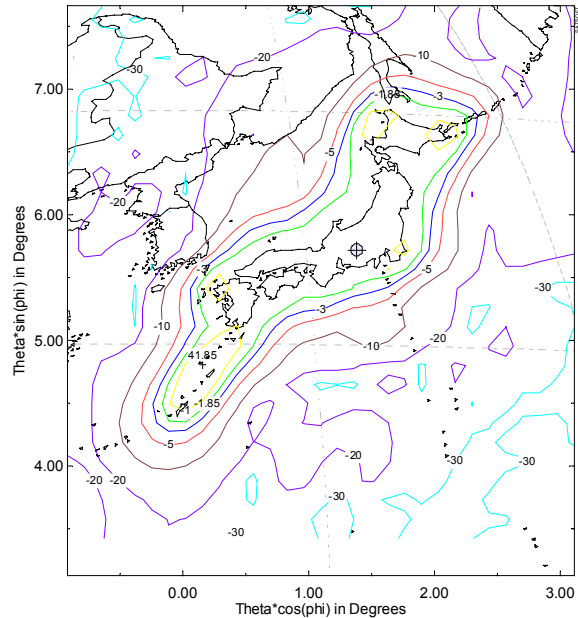
Four key changes are required to realize the necessary reflector performance improvements. Each item comprises a technology that has been fully developed, but all must be integrated into a full-scale AstroMesh™ reflector to validate the high-frequency design:

1. Denser nets: This relatively simple design change provides smaller, more numerous facets by increasing the number of webs and tension ties.
2. Graphite composite webs: An existing space-qualified material has been identified. It has been validated for coefficient of thermal expansion (CTE), stiffness, hysteresis and compatibility with existing manufacturing processes. More precise alignment of web manufacturing tooling will be performed to realize the full potential of this material.
3. High frequency mesh: This is a qualified product with flight heritage. RF tests have been performed at Ku-band, and are planned for a new configuration at Ka-band.
4. Shaped surface algorithms: New algorithms were developed for mesh reflector surface generation. RF performance and structural feasibility have been demonstrated analytically.

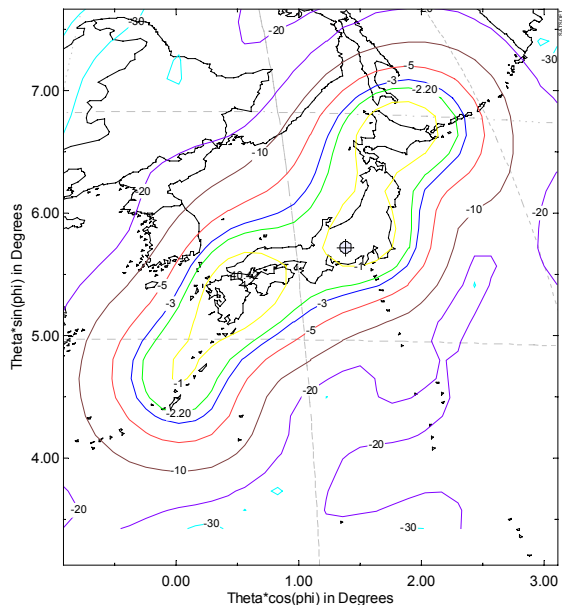
Shaped Reflector Examples

Shaped patterns for two Ku-band reflectors covering Japan are given in Figure 6. The solid reflector has an aperture of 2.5 meters, while the AstroMesh™ replacement has a 5.33-meter aperture. If both surfaces were perfectly formed, edge of coverage (EOC) directivity would be 38.22 dB and 40.0 dB respectively for an increase of 1.78 dB. The AstroMesh™ will incur an additional total loss of 0.22 dB for a minimum EOC improvement of 1.56 dB over the smaller aperture. Mesh reflector losses include 0.05 dB for

reflection, 0.06 dB for faceting and 0.09 dB from all other error sources as will be discussed.



5.33-Meter AstroMesh Gain Pattern



2.5-Meter Gain Pattern

Figure 6: Shaped Ku-Band Reflectors for Japan.

This analysis utilized a new, non-Zernike-based algorithm for surface generation. Development work has confirmed that the algorithm produces surfaces that are compatible with the reflector structure, and the engineering model will verify this. Further discourse about the theory, design

and performance of shaped AstroMesh surfaces is beyond the scope of this paper. To understand the gain loss values given for the above shaped AstroMesh™ example, however, we can apply the same trends that are suited to the parabola.

Parabolic Reflector Examples

The remainder of this paper will concentrate on a 6-meter offset parabolic circular aperture point-design with $F/d = 1.08$. Performance at Ku- and Ka-bands will be predicted by summing the total gain loss from all contributions. The major contributors for which losses will be estimated include mesh reflectivity and W_{RSS} surface errors. Surface error contributors are subdivided into faceting, manufacturing and thermo-elastic, pillowing, life and other material effects. The values reported herein account for numerous minute effects that are grouped within the principal categories.

Surface Approximation – Faceting Error

This type of error has been identified as a serious concern for higher frequency antennas due to the possibility that grating sidelobes will be produced. The following shows that although grating sidelobes are generated, they can be controlled to acceptable levels.

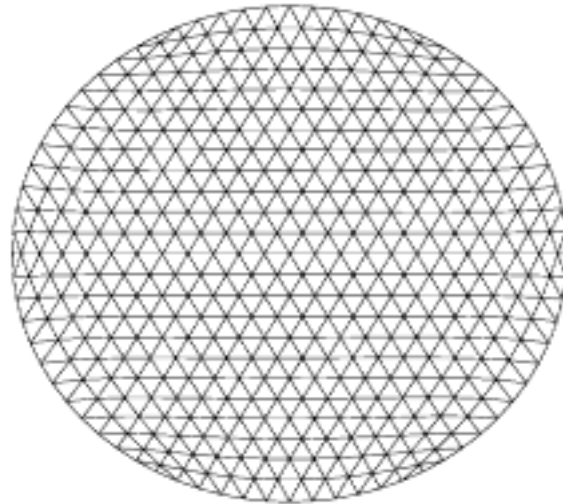
The first step in the design of an AstroMesh reflector is to determine the required facet size, and thus the number of rings from which the net and rim truss designs are derived. Faceting error is budgeted to be $W_{RSS}/3$ to yield the facet RMS, W_{FACET} . Maximum facet size is then calculated using the approximation³.

$$L = (F \cdot W_{FACET} / 0.0164)^{0.5} \quad (2)$$

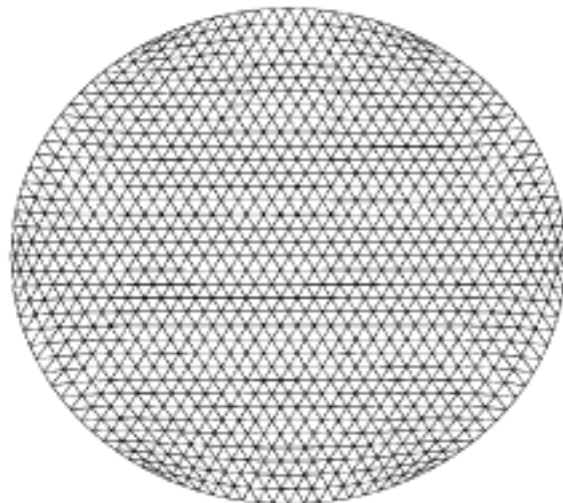
Where L is the average height of the triangular facet across the aperture plane and F is the focal length. This simple design methodology has been borne out by numerous RF analyses at various frequencies. It was used to derive an 18-ring net structure for the 6-meter Ka-band reflector point-design, and a 12-ring net structure for the Ku-band design. Existing AstroMesh™ reflectors have 10 rings with 600 total facets and 270 tie-points at the nodal intersections. The ring structures for both point-design surfaces are illustrated in Figure 7. Although the 18-ring Ka-band surface contains approximately 2000 facets and 1000 tie-points, it is within current capabilities. The 12-ring Ku-band surface has approximately 860 facets and 420 tie points.

The gain difference, ΔG_{FACET} , of 6-meter AstroMesh™ faceted surfaces compared to a smooth parabola is given in Figure 8 versus the facet ring quantity for operation at 30 GHz. The gain was calculated in two ways: one curve was

produced with detailed RF analysis using software proprietary to TRW, and the other using equation (1). The rigorously calculated losses for the periodically distorted surface show excellent agreement with Ruze yet are approximately 10 percent smaller.



12-Ring Structure



18-Ring Structure

Figure 7. 12-and 18-Ring AstroMesh Facet Designs.

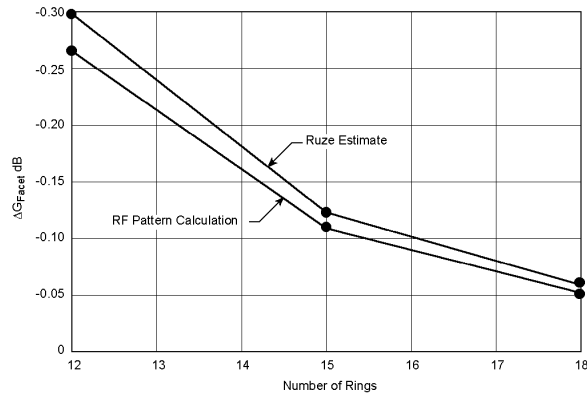


Figure 8. Facet Loss at 30 GHz.

As shown in Figure 9, peak gain from the calculated RF pattern is 64.75 dB, and ΔG_{FACET} is only -0.052 dB. As expected, the uniform periodicity of the surface directs the power lost in the main lobe into grating sidelobes. The pattern is pristine between the first lobes which are 32.32 dB down at ± 3.65 degrees azimuth. These grating lobes come and go with a 60-degree lattice periodicity as the cut is rotated about the zenith direction. The Ku-band pattern cut is shown in Figure 10. Peak gain is 58.12 dB, and ΔG_{FACET} is -0.062 dB. The first grating sidelobes are 31.2 dB down and ± 4.81 degrees off the boresight in azimuth.

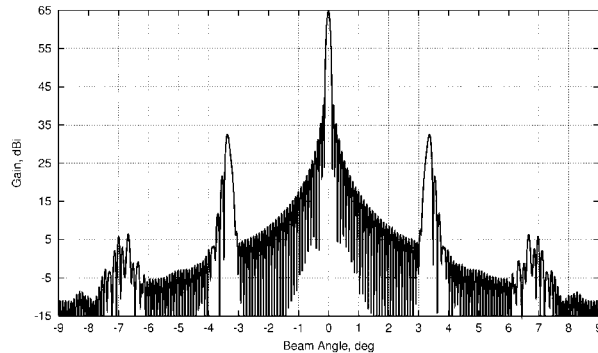


Figure 9. 18 Ring Surface at 30 GHz, Peak Gain = 64.752 dB.

Material and Manufacturing and Effects

All surface errors that are not systematic are grouped in this category. The effects include but are not limited to those from measurement and tooling accuracy, CTE and CTE scatter, strain scatter and hysteresis, stiffness, coefficient of moisture absorption (CME), creep, radiation and other life effects.

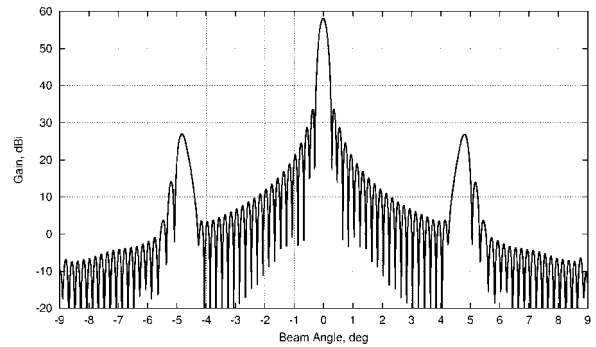


Figure 10. 12-Ring Surface at 14 GHz, Peak Gain = 58.124 dB

Truss rim errors are included in the manufacturing estimates. These errors are only 0.03 mm RMS for a 6-meter rim using current assembly methods. Rim truss CTE is matched to that of the webs, so thermal errors caused by the truss are limited. This type of performance is difficult to improve upon, so the newly developed graphite composite (GRP) web materials will be responsible for most of the surface accuracy improvements.

Material effects for the existing Aramid and new GRP web technologies are given in Table 1. In most cases the last column gives the ratio of the existing Aramid properties divided by the GRP properties. This gives a relative improvement ratio for the new web material. Improvements of the web axial stiffness and thickness, which affects surface roughness of the faceted surface, are handled inversely. The improvement ratios given in Table 1 represent a large increase in the surface accuracy potential of the new GRP nets.

When the size of one of the effects in Table 1 changes, the structural error that is coupled to it changes proportionally, or inversely, as with stiffness and vibration frequency⁴. Furthermore, the ratio W_{RSS}/d , where d is the average structural diameter, is useful for describing the accuracy potential of a given reflector technology. If sound scaling criteria are used, this ratio remains constant as the AstroMesh™ is scaled up or down in size. Extensive and detailed Monte Carlo simulations and hardware experience have verified these rule-of-thumb behaviors. They are provided not as a substitute for more explicit quantitative data, but to help the reader discern whether the following predictions are reasonable.

Table 2 gives a summary of all contributions to W_{RSS} with actual data from two existing reflectors, and with predictions for the point-designs. The manufacturing error data in the first row assumes that potential fixed pointing errors have been removed by alignment with the feed and spacecraft. Conversely, thermal pointing errors remain in the RMS error estimates in row 3. Each column of error categories is RSS summed to give a total W_{RSS} near the bottom row. As previously shown, random and systematic RMS errors have approximately the same affect on gain loss for this analysis. The impact of material and manufacturing effects on peak gain for the point-designs is given as ΔG_{MM} in the last row. This was calculated from equation (1) and W_{RSS} minus W_{FACET} . Note that pillowing is included in ΔG_{MM} , but it is always 1/8 of the faceting error, which makes its contribution to ΔG_{MM} insignificant.

All material and manufacturing effects that are responsible for the errors in each row of Table 2 are listed. The relative influence that the material effects have on the error categories is ranked by the order they appear in the fourth column. The

fifth column gives coarse estimates of material improvement factors. The improvement factors suggest the extent to which the GRP webs will contribute to improvement of surface errors.

Material and manufacturing error category performance of the 12-meter reflector can be compared to the 6-meter point designs by dividing by two to correct for diameter. The point design estimates can then be evaluated in light of the material improvement factors. Several of the point design material and manufacturing error estimates are seen to be significantly higher than what might be justified by the relevant improvement factors. The overall point-design error predictions are thus conservative.

Mesh Reflection Losses

Predicted and measured reflection losses for three different types of mesh are given in Figure 11. The predictions are based on RF analysis of detailed finite element models of mesh structures.

Table 1: Web Material Effects

Effects	GRP (μ strain)	Aramid (μ strain)	Aramid/GRP Ratio
A) CTE	-0.155/ $^{\circ}$ C	-1.08/ $^{\circ}$ C	7.0
B) CTE scatter	\pm 0.03/ $^{\circ}$ C	\pm 0.30/ $^{\circ}$ C	10
C) Hysteresis	20	300	15
D) CME	15	220	14.7
E) Manufacturing	0.7 RMS	1.1 RMS	1.6
F) Creep	20	200	10
G) Other life effects	20	40	2.0
H) Thickness	Thickness reduced by 1/2		2.0
I) Axial modulus	Stiffness increased 4 x		4.0

Table 2: Reflector W_{RSS} and Gain/Loss from Material and Manufacturing Effects

Surface Error Contribution (mm, RMS)	ACTUAL PERFORMANCE		Material Effects & Rank	Weighted Improvement Factor	PREDICTED PERFORMANCE	
	6-meter DM(mm, RMS)	12-meter Flight (mm, RMS)			Ku Point-design (mm, RMS)	Ka Point-design (mm, RMS)
Manufacturing	0.40	0.40	C, D, E, I, B, A	12x	0.13	0.13
Orbital thermal	0.25	0.60	A, B	8x	0.08	0.08
Repeatability, life & gravity effects	0.08	0.16	F, G, I	5x	0.04	0.04
Facet surface roughness	0.15	0.15	H, E	2x	0.075	0.075
W_{FACET} (systematic)	0.36	1.15	-	-	0.17	0.08
Pillowing (systematic)	0.05	0.14	-	-	0.021	0.01
TOTAL W_{RSS}	0.62	1.38	-	-	0.245	0.192
PREDICTED ΔG_{MM} (dB)					-0.09	-0.21

Measured data was taken in controlled tests at frequencies of 5, 12, 14, 18, 22, 26 and 30 GHz with flat samples that were at least 0.5 meters on each edge. Reflection loss was measured indirectly by measuring transparency through the material. This leakage was measured for incidence angles of 60 degrees to 90 degrees, which is larger than the incidence angles of the antennas that are being discussed. The highest losses were apparent at 90 degrees, so only that data is presented. Equivalent results were achieved in several tests that measured reflectivity directly. These more difficult tests corroborated the transmission loss measurements. No unexpected scatter was seen in any reflection measurement.

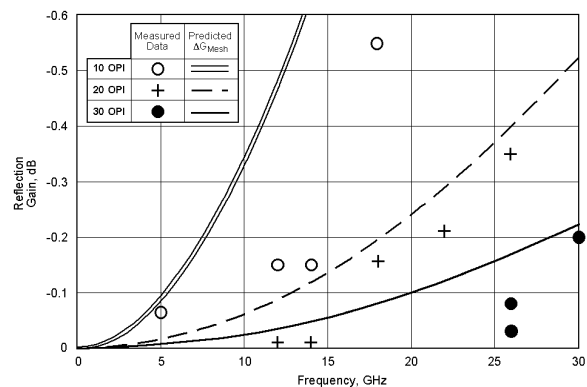


Figure 11. Mesh Reflection Loss.

All testing between 12 and 26 GHz was performed with co-polarized signals. The principal and cross polarization reflection patterns from the mesh samples were compared to those of a “perfect” metallic plate reflector. This test gives an accurate assessment of cross-polarization generation. No significant deviations in the reflected patterns were noted, and circularly polarized signals were not tested.

All measured data shown in Figure 11 is below the predicted mesh reflection losses. The term ΔG_{MESH} in the following summary of overall Ku- and Ka-band reflector performance will therefore be based on the more conservative predictions.

Summary of Results

Table 3 summarizes reflector gain/loss predictions for the point designs. Total predicted loss is given in the last row of the Table is about -0.2 dB and -0.48 dB for the Ku- and Ka-Band reflectors, respectively.

Table 3: 6-meter Point Design Reflector Gain/Loss Summary

Gain Source	Ku-band Reflector Gain (dB)	Ka-band Reflector Gain (dB)
ΔG_{FACET}	-0.062	-0.052
ΔG_{MM}	-0.09	-0.21
ΔG_{MESH}	-0.05	-0.22
ΔG_{TOTAL}	-0.20	-0.48

Conclusions

The maximum goal of less than 0.30 dB loss was exceeded by the Ku-band point-design reflector. This also confirms that excellent shaped reflector surface performance is within reach for large deployable Ku-band apertures using current AstroMesh technology. This will be confirmed with tests on the 6-meter engineering model this year. Ku-band reflector performance

The excellent performance displayed by these Ku- and Ka-Band reflectors must be equaled by the deployment booms that are required for deploying and supporting them from a spacecraft. Existing flight hardware should be able to meet this challenge.

at 6-meters shows that satisfactory performance with a 12-meter aperture diameter is feasible.

Performance at Ka-band missed the stated goals, but the performance does show that grating sidelobes due to surface periodicity can be controlled. It is anticipated that in practice, such small grating lobes will be masked by the sidelobes produced by random surface errors. Current testing shows that new mesh being developed for flight may reliably display reflection losses that are closer to -0.1 dB at 30 GHz than the analytically predicted -0.22 dB. If so, the peak gain loss of a 6-meter Ka-band reflector would be about -0.40 dB with the current technology. This may be adequate considering that the grating sidelobes are small and peak gain is well over 64 dB. A smaller aperture will produce proportionally smaller total gain loss from all sources except the mesh.

Beam pointing provides a mitigating factor that may make the performance of both reflectors appear more attractive. For instance, much of the orbital thermal distortion given in Table 2 involves global shape changes that affect pointing more than surface roughness. Thus, if the spacecraft is able to adjust antenna fine pointing with body steering or other automatic tracking capability utilizing a secondary or swash plate, for instance, these diurnal deviations would be easily removed.

¹ Utku, S., and Barondess, S.M., Computation of weighted Root-Mean-Square of Path Length Changes Caused by the Deformations and Imperfections of Rotational Paraboloidal Antennas, Technical Memorandum 33-118, Jet Propulsion Laboratory, Pasadena CA, March 1963.

² Ruze, John, "Antenna tolerance theory – A Review" Proceedings of the IEEE, Vol. 54 pages 633-640, April 1966.

³ Hedgepeth, J. M. Accuracy Potentials for Large Space Antenna Reflectors with Passive Structure. Journal of Spacecraft and Rockets 19,3 (1982), 211-217.

⁴ Hedgepeth, J.M., Influence of Fabrication Tolerances on the Surface Accuracy of Large Antenna Structures. AIAA Journal Vol. 20, No. 5, (1982), pgs. 680-686.